Proceedings of Lasers'95
Charleston, SC - December 4-8, 1995

CONF-951275--3
BNL-62846

INVERSE CHERENKOV AND INVERSE FEL ACCELERATOR EXPERIMENTS AT THE BROOKHAVEN* ACCELERATOR TEST FACILITY

I.V. Pogorelsky, A.vanSteenbergen, M. Babzien, I. Ben-Zvi, R. Fernow, J. Gallardo, K.P. Kusche, T. Srinivasan-Rao, and X.J. Wang
Accelerator Test Facility, Brookhaven National Laboratory, Upton, NY 11973

W.D. Kimura, G.H. Kim, and R.D. Romea
STI Optronics Inc., 2755 Northup Way, Bellevue, WA 98004

Y. Liu, and D. Cline
Physics Department, UCLA, Los Angeles, CA 90024

J.R. Fontana
University of California, Santa Barbara, CA 93106

A. Fisher
Stanford Linear Accelerator Center, Stanford, CA 94309

J. Sandweiss
Yale Univ. New Haven, CT 06520

X. J. Qui
SUNY at Stony Brook, Stony Brook, NY 11794

J-M. Fang
Columbia Univ., New York, NY 10027

Abstract

Status update on the ongoing inverse Cherenkov acceleration experiment and prospects to its 100 MeV short-term upgrade. The first report on 1 MeV electron acceleration with the 0.5 GW CO_2 laser used in the inverse FEL scheme.

I. Introduction

The fundamental motivation for studying laser driven accelerators is the extremely high fields attainable upon focusing of high-peak-power laser beams. With state-of-the-art lasers, as high as ~1 TV/m transverse electric fields may be attained. The question is how to convert at least a fraction of this enormous field into the effective longitudinal accelerating field.

According to Lawson-Woodward theorem,[1] no net particle acceleration is possible using any superposition of electromagnetic (EM) waves in free space. However, there are a number of ways to utilize lasers for particle acceleration if not exactly in a free space.

In general, all laser accelerator schemes may be split into three major categories: far EM field, near EM field, and plasma accelerators. How to define the border between the first two methods? EM field may be presented as a sum of propagating EM waves

$$\vec{E}(\vec{x},t) = \sum_j A_j \exp\left[i\left(\vec{k}_j \times \vec{x}_j - \omega_j t\right)\right]. \quad (1)$$

When all wave vectors $\vec{k}_j$ are real, we talk about far field accelerators. For these schemes it is essential for the distance from the source of far fields or from any boundary surface to be >>λ. Otherwise, near field effects may become of relevance. Fields with imaginary $\vec{k}_j$ are called near fields. Actually, in this case, we talk about evanescent fields vanishing within a one-wavelength-thick layer above the surface. In the third group of methods, particles are accelerated not by EM fields but by electrostatic fields due to the charge separation in laser-induced plasma waves.

The study of any scheme has the primary practical goal of finding an alternative to conventional accelerators in order to build, in the future, more economical high-energy (~TeV) machines, or compact moderate-energy (~GeV) accelerators. So far, the record ~40 MeV over a 0.5 cm distance, laser acceleration has been demonstrated using the plasma wakefield method[2]. However, all different kinds of methods are under consideration and study.

*This work was performed under the auspices of the U.S. Department of Energy.

At the Brookhaven Accelerator Test Facility (ATF), we have a unique opportunity. There are already two far-field accelerator experiments producing results. These are: Inverse Cherenkov Accelerator (ICA)[3-5] and Inverse Free Electron Laser (IFEL) accelerator[6,7]. In addition to it, a near field Grating Linac[8,9] is scheduled for tests, and a plasma acceleration experiment is considered for initiation.[10,11]

In this paper, we present the latest results obtained during the ICA and IFEL experiments.

II. ATF Overview

The ATF is a users' facility at Brookhaven National Laboratory that provides a high brightness electron beam and high power laser pulses synchronized to the electron beam. The 10-ps bunch of electrons is produced by a laser photocathode electron gun and is accelerated to 70 MeV in the RF travel-wave linac.[12] The laser system consists of Nd:YAG[13] and CO_2 lasers[14,15].

20 mJ, 15-ps pulses are produced by the Nd:YAG laser in a 3 Hz sequence. Part of this energy is directed through the second and then 4th harmonic crystal to a photocathode generating 10-ps electron bunches with a charge of ~1 nC. Other portion is split to control picosecond slicing[16] in the CO_2 laser system, thus ensuring synchronization of electron bunches with high-power pulses of IR radiation delivered by the CO_2 laser.

In principle, the sliced CO_2 laser pulse may be as short as the electron bunch. However, a low level for the pulse duration is presently set by the CO_2 laser amplifier bandwidth that depends upon the amplifier gas pressure. Presently, we use 3-atm UV-preionized amplifier. The inverse Fourier transform of its pressure-broadened rotational spectrum gives 50 ps. The shortest pulse that we can efficiently amplify turns out to be approximately twice that. Pulses delivered from the multipass amplifier have ~1 J energy, corresponding to 10 GW of peak power.

To test different accelerator schemes, the CO_2 laser beam is transported to several locations in the experimental hall where it interacts with e-bunches produced by the linac. Presently two laser acceleration experiments are active: ICA and IFEL located in two parallel electron beam-lines in the ATF experimental hall (see Fig.1).

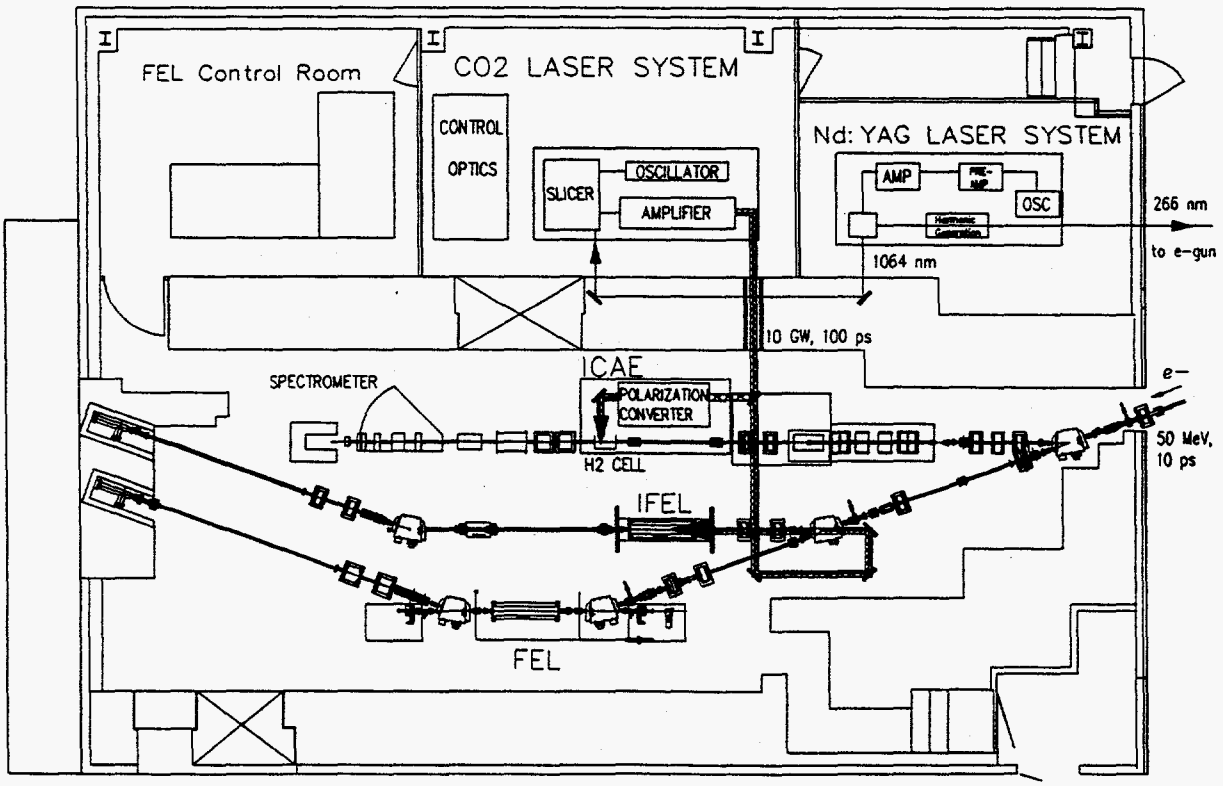

Fig.1. Brookhaven Accelerator Test Facility

Before reaching the interaction point, the laser beam travels over ~20 m distance. For the IFEL experiment, the beam is telescoped and coupled into a 2.8-mm diameter sapphire guide. On the ICA optical table, the initially linearly polarized CO_2 laser beam undergoes transformation to radial polarization in the interferometer aligned with subwavelength accuracy and, then,

is focused along the e-beam propagation with a positioning and angular accuracy of ~20 μm and 0.1 mrad, respectively. All this is possible due to the high laser beam coherence, quality, pointing stability and low divergence specified in the table insert in Fig.2. The efficient coupling of the e-beam within the laser focus regions for both experiments is possible due to the high stability and low emittance (ε_n=2 mm.mrad, normalized) inherent in the ATF linac and the e-beam transport system.[12] Timing control between the electron bunches and laser pulses is done for both experiments by adjusting an optical delay line.

Details and the most recent results of the ICA and IFEL experiments are presented in the next two Sections.

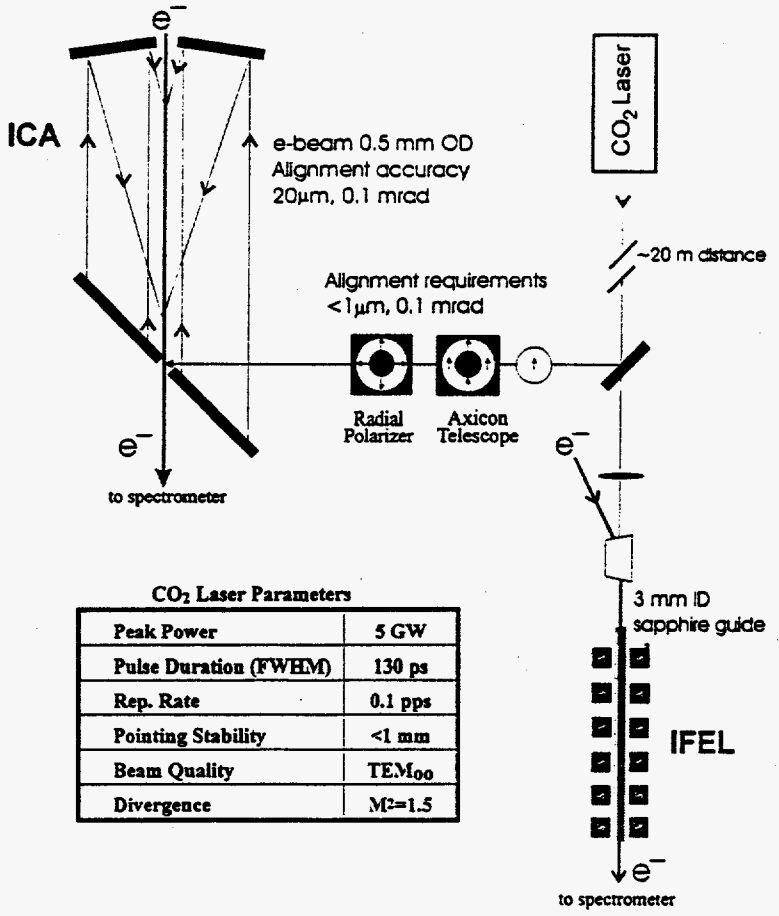

CO_2 Laser Parameters

Peak Power	5 GW
Pulse Duration (FWHM)	130 ps
Rep. Rate	0.1 pps
Pointing Stability	<1 mm
Beam Quality	TEM_{00}
Divergence	M^2=1.5

Fig.2. CO_2 laser beam delivery to the ICA and IFEL experiments

III. Inverse Cherenkov accelerator

In any laser acceleration scheme, the key question is how to maintain synchronism between particles and oscillating electric fields over an appreciable distance. One of the possibilities is when the particle, traveling with velocity βc, and the wavevector cross in a medium at an angle θ (known as Cherenkov angle) which is described by the condition

$$\cos\theta = 1/\beta n. \qquad (2)$$

Inverse Cherenkov acceleration is the only example of a first order, far field acceleration process where the particle interacts just with one EM wave. Here, the inclination of the wavevector is responsible for developing a longitudinal accelerating field, while the medium produces retardation of the phase velocity of the wave to match the speed of electrons.

In the first ICA demonstration[3], a linear polarized, focused Nd laser beam crossed the path of the electron beam in the interaction cell filled with hydrogen. The observed energy shift was 50 keV over a 7 cm interaction length.

In the modified scheme[4] (see Fig.3b) which is under test at the ATF, we start with a radially polarized beam. By an axicon, the laser beam is converged to the e-beam axis, *z*, producing a cylindrically symmetrical interference pattern. Radial field components cancel at the axis and J_1-type Bessel interference field, shown in Fig.4a, develops:

$$E_r(r,z) = E_0(z) J_1(2\pi r\theta/\lambda), \tag{3}$$

where $E_0(z)$ is a field amplitude that depends upon the laser intensity distribution at the axicon surface, $W(R)$,

$$E_0(z) = 2\pi\theta\sqrt{\frac{2zW(R)}{\varepsilon_0 c\lambda}}. \tag{4}$$

A longitudinal component of the electric field, which is responsible for accelerating electrons, can be expressed analytically by a Bessel function of the first kind of the order 0:

$$E_z(r,z) = tg\theta \times E_0(z) J_0(2\pi\theta r/\lambda), \tag{5}$$

This distribution has a maximum along the z axis. The amplitude of this component corresponds to the peak acceleration gradient attainable under the phase matching condition, Eq.(2). The radial position of the first minimum in the distribution Eq.(5) is at

$$r_{max}=0.38\lambda/\theta; \tag{6}$$

for λ=10.6 μm and θ=20 mrad, $r_{max}\approx$200 μm.

The axicon geometry has several advantages over the arrangement used in the Stanford experiment. It produces more efficient coupling of laser energy to the e-beam. The E_r component can also focus the e-beam. This may help to mitigate some of the detrimental effects of gas scattering by channeling the electrons in the longitudinal direction.

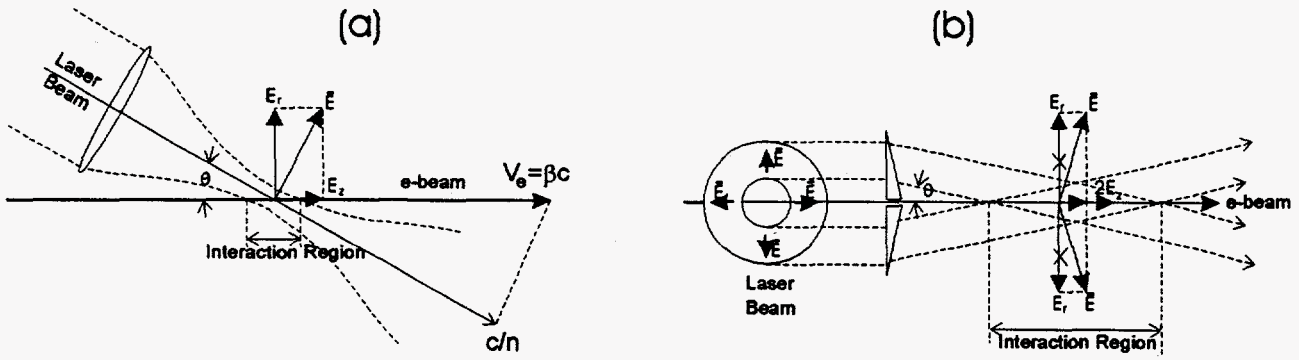

Fig.3 ICA principle and the first experimental demonstration (a); axicon geometry(b)

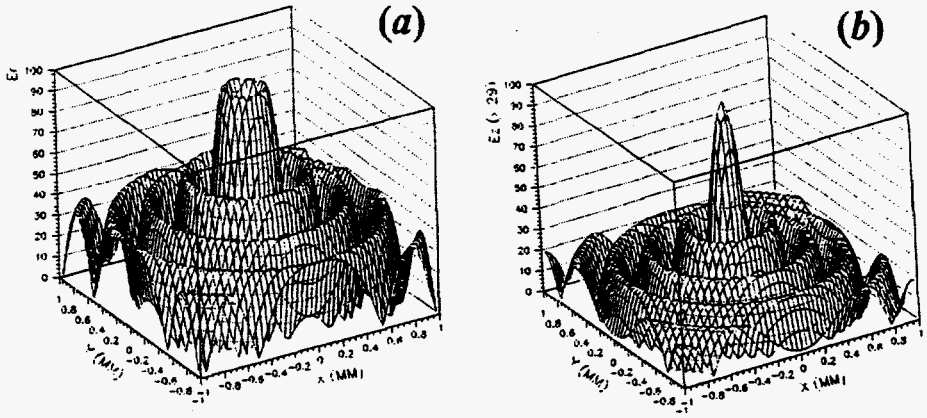

Fig.4 Radial distributions of the radial (a) and longitudinal (b) electric field components in the axicon-focused laser beam.

The major components of the experiment are: an optical system for converting the linearly polarized CO_2 laser beam into one with radial polarization; a gas cell where the ICA interaction occurs, an electron beam transport line connected to the gas cell, and optical and e-beam diagnostics. Fig.5 shows a schematic layout of the optical system.

The radial polarization converter system utilizes a double Max-Zander interferometer technique.[17] The laser beam enters the cell through a ZnSe window, it reflects off a 45° mirror, and sent to the axicon mirror which performs the same function as the lens in the diagram on Fig.3b. In the ATF experiment, the axicon angle is θ=20 mrad. At the initial electron energy 50 MeV, the phase-matching Cherenkov condition, Eq.(2), is satisfied by having 2.2 atm of hydrogen in the interaction cell.

To introduce the e-beam to the interaction region, the axicon mirror has a 0.5 mm diameter hole drilled in the center. This aperture defines the e-beam diameter that matches the width of the accelerating fields radial distribution as according to Eq.(6). The length of the interaction region depends upon the axicon angle and the input beam diameter and was ~12 cm in the course of the ATF experiment. The 45^0 mirror has a 1.0-mm diameter hole drilled for the e-beam to travel through. The electrons enter and exit the gas cell through 2-μm thick diamond windows of a 1×1 mm^2 aperture, which separate the pressurized cell from the high-vacuum beam pipes.

The center of the Bessel distribution produced by the axicon is brought to a coincidence with the e-beam propagation axis, *z*, with the transverse and angular accuracy of several microns and a fraction of a milliradian, correspondingly. This can be done by using remote-controlled motormikes, which adjust the axicon mirror tilt, and pop-in screens and a high-magnification IR/visible TV imaging system placed in the spent CO_2 laser beam.

An electron energy spectrometer is located downstream from the ICA gas cell and, together with the strip-line charge monitor, is the primary diagnostic during the experiment. Fig.6 presents the rough images observed at the spectrometer phosphor screen in the course of the ICA experiment. Since the electron bunch length is much longer than the laser wavelength, the interaction between the e-beam and the laser beam occurs over all phases of the laser light wave, resulting in both accelerated and decelerated electrons being observed. The spectrometer has a momentum acceptance range of ~±2% of the mean energy. Since the ICA interaction resulted in energy modulation much larger than this range, it was necessary during the experiment to scan the spectrometer. Up to 3.7 MeV maximum acceleration has been measured when less than 1 GW CO_2 laser power was delivered to the interaction region.

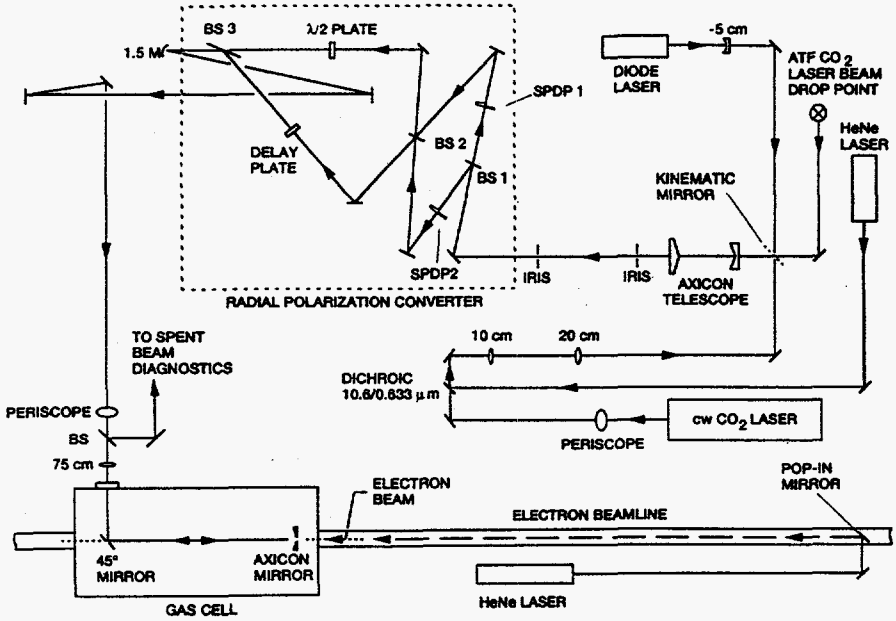

Fig.5 Schematic plan view of the ICA optical setup

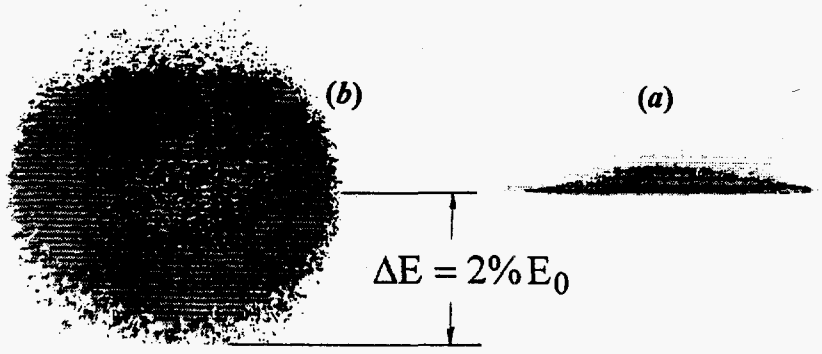

Fig.6 Snap-shots of the electron spectrometer screen without laser (a) and with ~1-GW laser pulse delivered to the ICA cell (b)

In order to proceed to the demonstration of stronger acceleration at higher laser power, several problems shall be addressed including: gas and optics breakdown and the limited acceptance angle of the downstream e-beam diagnostics. After the completion of the ongoing ATF CO_2 laser upgrade to a 3 ps pulse duration, as high as 200 GW laser peak power may be delivered into the existing gas cell before the gas breakdown or optics damage occurs.[18] A Monte-Carlo computer simulation of the ICA process shows a possibility of a 100 MeV acceleration demonstration over a 30 cm long interaction range corresponding to the acceleration gradient of 333 MeV/m.[19] The acceleration efficiency will be improved by ensuring better phasing of the electrons with the accelerating field. For this purpose, periodical electron prebunching with the spatial interval equal to the laser wavelength will be produced in a low-power ICA cell placed before the high-power accelerator cell.

III. IFEL Experiment

The IFEL scheme is an example of a second order, far field laser acceleration process. In this case, a second field of a wiggler magnet is used to bring the relativistic particles into a transverse oscillating motion. Thus, transverse EM laser field has a projection of its electrical component along the local direction of the e-beam propagation. Hence, electric forces may produce an additional kick to the electrons in the direction of their propagation, provided the laser field is in phase with the electron wiggling.

In vacuum, the oscillating electron can not propagate with a phase velocity of light along the direction of the laser beam. Now, synchronism means that the electron should slip exactly one period (or integer number of periods) of the EM wave while traveling a wiggler period, λ_w. The synchronism condition at a small angle limit takes the form

$$\lambda = \frac{\lambda_w}{2\gamma^2}\left(1+K^2\right) \tag{7}$$

where K is a dimensionless wiggler parameter equal to $K = \frac{eB_w\lambda_w}{2\pi mc^2}$ and B_w - wiggler magnetic field. Hence, the condition (7) may be satisfied by adjusting wiggler field and period.

For the set of parameters of the ATF IFEL experiment, a reasonable estimate of the energy gain by the electron beam in a wiggler of length L_w is given by

$$\Delta E = \frac{eE_L}{2\gamma_{in}} Kf(K) L_w \sin\psi_r, \tag{8}$$

where E_L is the laser electric field amplitude, γ_{in} is the initial electron energy relativistic factor, ψ_r - the resonance phase ($\approx 45^0$ for maximum bunch size), and $f(K)\approx 0.4$.

First proposed by Robert Palmer in 1972,[6] IFEL acceleration has been demonstrated in Yerevan Physics Institute (Armenia) in 1990 using a 12-MeV electron beam with a 20-MW CO_2 laser.[20] The maximum observed energy gain in a 20 cm wiggler was 20 keV.

In a later experiment at Columbia University,[21] 750 keV electron beam was used. The e-beam passed through two wigglers. The first wiggler was used as FEL to generate power for the acceleration process. The second 37 cm long wiggler, which was used for IFEL, had a tapered period of a 1.8-2.25 cm and a field strength of 400 G. 10% of the injected electrons were accelerated to a maximum energy of 1 MeV.

The goal of the ATF IFEL experiment is further optimization of the accelerator parameters. Table 1 presents design parameters for the first stage of the IFEL experiment when a 5 GW CO_2 laser is used. In addition to the higher laser power used in this experiment, other optical issues are also carefully addressed. The laser beam is guided inside a low-loss sapphire waveguide of 2.8 mm diameter mounted inside a 4 mm gap of a 0.5 m-long wiggler. The guide maintains stable laser beam conditions through the whole wiggler length. This concept is also relevant to the future long, multi-stage accelerators.

Another novel feature of the ATF IFEL is a special design of a variable period, fast excitation wiggler[22] illustrated in Fig.7. The wiggler is structured from a stack of interleaving, 0.25 mm thick Vanadium Permandur ferromagnetic laminations. The laminations are assembled in $\lambda_w/4$ groups. These are separated by $\lambda_w/8$ thick Cu sheets that act as field reflectors and enhance the strength of the magnetic field two times. Altering the period tapering is an easy operation. The magnet is energized with a 6 kA, 300 μs current pulse transmitted through four Cu rods penetrating the laminations. The design is characterized by a high field strength and a possibility to vary tapering to ensure synchronism of the accelerated electrons with the laser wave.

The observations of the e-beam spot on a phosphor screen at the dipole spectrograph demonstrate the IFEL effect. Fig.8 presents scans taken across the two-dimensional intensity distributions. We see how electrons are efficiently trapped and accelerated. Because of problems with vacuum degradation when the laser is delivered inside the guide, the laser power was kept below 0.5 GW. Observed acceleration is 2.2%. Further optimization is under way.

Near term plans call for increasing the CO_2 laser power to 200 GW. This should give an accelerating gradient of 100 MeV/m.

Table 1. Design Parameters for IFEL Experiment

Wiggler	
Length [cm]	48
Period [cm]	2.89-3.14
Gap [cm]	0.4
Field [T]	1.0
Electron Oscillation [mm]	0.16-0.19
CO_2 Laser Driver	
Peak Power [GW]	4.4
Max. Field, E_0 [GV/m]	1.63
Waveguide Losses [m^{-1}]	0.05
Electron Beam	
Injection Energy [MeV]	40.0
Projected Exit Energy [MeV]	45.8
Projected Mean Accel. Field [MV/m]	12.3
Beam Radius [mm]	0.3
Normalized Emittance [mm.mrad]	5
e^-/Bunch	10^9

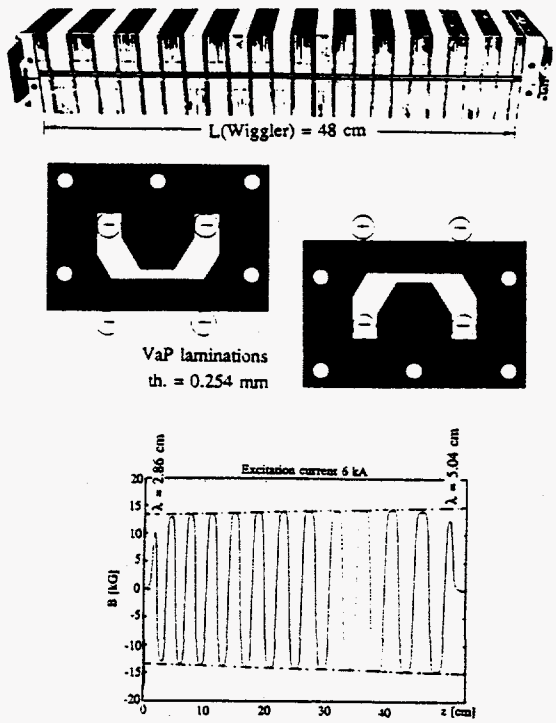

Fig.7 IFEL fast excitation, tapered period wiggler L_w=48 cm, Gap= 4 mm, V=400 V, Induct=5 μH

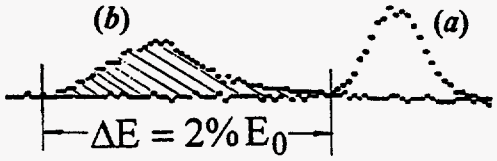

Fig.8. Electron beam distributions obtained on a phosphor screen placed downstream of the dipole bending magnet at the end of the IFEL beamline:(a) no laser; (b) with 0.5 GW laser power; E(linac)=40 MeV, B_w=10 kG, λ_w=2.9-3.1 cm.

IV. Conclusions

Two far field laser electron accelerator schemes are under test at the ATF. The improved axicon geometry for the inverse Cherenkov acceleration has been demonstrated. The record for far field schemes, 3.7 MeV acceleration has been obtained. According to simulation, near term experiments should produce up to 10 MeV acceleration.

The improved IFEL scheme features a high-power laser beam guided inside the fast excitation, variable period wiggler. During the first test of this scheme, with a 0.5 GW of a CO_2 laser power, 1 MeV electron acceleration has been observed. Upon the optimization of the process parameters, 6 MeV acceleration, at 5 GW CO_2 laser power, is predicted by simulations.

A 10-GW CO_2 laser available at the ATF is powerful enough for initial proof-of-principle laser acceleration experiments. However, for more advanced experiments much higher laser power would be needed. For instance, both far-field laser accelerator schemes that are under test at the ATF are potentially scalable to 100 MeV. To reach this milestone, about 200 GW CO_2 laser will be needed. To meet these requirements a 4 TW, 3 ps CO_2 laser system is under development at the ATF.[11] Expanding the capabilities of the state-of-the-art picosecond terawatt laser technology, the upgraded laser will provide an opportunity to study a variety of laser acceleration methods in the medium-IR region.

References

1 R.B Palmer, *Particle Accel.*, **11**, 81 (1980)

2 A.E. Dangor, "The Breaking of Relativistic Electron Plasma Waves", *Symposium on Short Pulse lasers and Wakefield Accelerators, 37th Anual Meeting of the Division of Plasma Physics, APS*, November 6-10, 1995, Louisville, Kentucky

3 J.A. Edighoffer, W.D. Kimura, R.H. Pantell, M.A. Piestrup, and D.Y. Wang, *Phys. Rev.*, **A23**, 1848 (1981)

4 J.R. Fontana and R.H. Pantell, *J. Appl. Phys.*, **54**, 4285 (1983)

5 W.D. Kimura, G.H. Kim, R.D. Romea, L.C. Steinhauer, I.V. Pogorelsky, K.P. Kusche, R.C. Fernow, X. Wang, and Y. Liu, *Phys. Rev. Lett.*, **74**, 546 (1995)

6 R.B Palmer, *J. Appl. Phys.*, **43**, 3014 (1972)

7 A. Fisher, J. Gallardo, J. Sandweiss, and A. van Steenbergen, *Proc. Advanced Accelerator Concepts*, Port Jefferson, NY, 1992, AIP, **279**, 299 (1993)

8 R.B. Palmer, *Proc. Laser Acceleration of Particles*, AIP., **91**, 179 (1982)

9 R.C. Fernow and J. Claus, *Proc. Advanced Accelerator Concepts*, Port Jefferson, NY, 1992, AIP, **279**, 212 (1993)

10 S.V. Bulanov, T.J. Esirkepov, N.M. Naumova, F. Pegoraro, I. Pogorelsky, and A.M. Pukhov, "Controlled Wake Field Acceleration via Laser Pulse Shaping", *IEEE Trans. Plasma Sci.*, April 1996 (to be published).

11 I.V. Pogorelsky, "Relativistically Strong CO_2 Laser Driver for Plasma-Channeled Particle Acceleration", *Proc. Lasers'95*, Charleston, SC (1995)

12 I. Ben-Zvi, *Proc. Advanced Accelerator Concepts*, Port Jefferson, NY, 1992, AIP, **279**, 590 (1993)

13 A. Fisher, M. Babzien, I. Pogorelsky, T. Srinivasan-Rao, High-Stability Nd:YAG Photocathode Driver Laser" CLEO 95, Baltimore, MD, May 21-26, 1995 (to be published).

14 I. Pogorelsky, J. Fischer, A.S. Fisher, T. Srinivasan-Rao, N.A. Kurnit, I.J. Bijio, R.F. Harrison, T. Shimada, K. Kusche, and M. Babzien, *Proc. Lasers'93*, Lake Tahoe, NV, 647, (1994)

15 I.V. Pogorelsky, J. Fischer, K. Kusche, M. Babzien, N.A. Kurnit, I.J. Bijio, R.F. Harrison, and T. Shimada, *IEEE J. Quant. Electron.*, **31**, 556 (1995)

16 P.B. Corkum, *IEEE J. Quant. Electron.*, **QE-21**, 216 (1985).

17 S.C. Tidwell, G.H. Kim, and W.D. Kimura, *Appl. Opt.*, **32**, 5222 (1993).

18 Y. Liu, I.V. Pogorelsky, W.D. Kimura, and D. Cline, "Inverse Cherenkov Laser Accelerator Upscaling to Gas Breakdown Limit", submitted to *Nucl. Instrum. and Methods in Phys. Res.*

19 W.D. Kimura, R.D. Romea, and L.C. Steinhauer, "Inverse Cherenkov Acceleration and Scaling to TeV Accelerators", *Particle World*, (to be published).

20 A.T. Amatuni et al, *Part. Accel.*, **32**, 221 (1990).

21 I. Wernick and T.C. Marshall, *Proc. Advanced Accelerator Concepts*, Port Jefferson, NY, 1992, AIP, **279**, 292 (1993)

22 A. vanSteenbergen, US Patent **#368618**, 1990